

Study the Effect of the Friction Stir Process on the Microstructure and Mechanical Behavior of the AZ31 As-cast Alloy Joint

Amir Rezaei¹, Iman Ebrahimzadeh^{1,*}, Farhad Gharavi²

¹ Advanced Materials Research Center, Department of Materials Engineering, Najafabad Branch, Islamic Azad University, Najafabad, Iran.

² Department of Material Engineering, Sirjan Branch, Islamic Azad Univeristy, Sirjan, Iran

ARTICLE INFO

Article history:

Received 3 March 2019

Accepted 30 September 2019

Available online 1 November 2019

Keywords:

AZ31 Casting (Az-cast) Alloy
Friction Stir Process (FSP)
Gas Tungsten
Arc Welding (GTAW)
Mechanical Properties
Microstructure

ABSTRACT

The AZ31 magnesium alloy has a significant potential for the aircraft manufacturing industry due to its low density and proper mechanical properties. In this research, the Gas Tungsten Arc Welding (GTAW) process was used by applying pulse current for the AZ31 as-cast alloy joint. Then, the effect of frictional stir process (FSP) on the microstructure and mechanical properties of this joint was examined. Subsequently, the friction stir process was performed with a tool rotating speed of 1120 rpm, the tool traverse speed of 50 mm/min in two passes behind and on the welding line. The microstructure and fracture sections of the prepared samples were respectively examined by optical microscopy and scanning electron microscopy (SEM). The mechanical behavior of the samples was studied using tensile, micro-hardness and impact tests. According to the results, the microstructure of the welding region of the TIG sample included highly fine homogeneous and coaxial grains. After the friction stir process (FSP), the microstructure transformed into fine and structural grains in the form of a ring-shaped morphology. The FSP resulted in a 23% improvement in the tensile strength of the TIG sample. Also, the impact energy of the welding metal increased by about 37%. In general, the mechanical behavior of the joint was improved after applying the friction stir process.

1-Introduction

One of the most important modern needs of the world is the use of light metals in the aerospace and automotive industries due to the fuel economy [1-3]. Due to good strength and light weight, low surface tension, high chemical activity, and high thermal conductivity, the magnesium alloys are widely used in the automotive and aircraft industries [4-6]. Magnesium alloys are lightweight alloys that have replaced aluminum and steel because of their proper properties such as low density (36% lower than aluminum and 78% less than steel)

and high specific strength [7 & 8]. Previous studies have shown that the welding by these alloys is associated with some problems like intense tendency to oxidation, high heat conduction, low melting and boiling temperatures, solid contraction and the tendency to form low melting particles, low viscosity, and high solubility for hydrogen in the liquid state due to low physical properties of magnesium [9 &10]. One of the most important of these problems is the cracking sensitivity and the formation of coarse grains in the welding process [11]. The friction stir process (FSP) is a

* Corresponding author:

E-mail address: i.ebrahimzadeh@pmt.iaun.ac.ir

thermo-mechanical process, in which, both the mechanical and thermal aspects control the process and, consequently, the microstructure and mechanical properties of the material [12]. The size of grains reduces in this method due to the mechanical recrystallization. One of the most important goals of industrial designers is to choose a suitable connection method and a proper secondary process to improve the microstructural and mechanical behaviors aimed at making the best use of the existing state of the parts [13]. The Friction Stir process (FSP) was developed as a method based on the principles of friction stir welding since 1991 [14]. This process is used to improve and control the microstructures in the layers close to the surface of the processed metal compounds to promote specific features [15]. This process has been proven nowadays to be a far more effective method to achieve fine-grained structure and uniformity in the processed area and eliminate the defects from the manufacturing process in comparison with other methods. The FSP process improves the characteristics such as hardness, tensile strength, yield strength, fatigue, and the wear resistance. The microstructures formed have been recrystallized with homogeneous coaxial grains and improved the superplastic behavior [15].

Damir et al. [16] studied the TIG welding of AZ31 magnesium alloy sheets using two alternating and pulse currents. The results indicated that the AZ31 magnesium alloys can be welded well using the TIG welding method. The microstructure of samples welded by pulse current contained finer and more coaxial grains compared to the samples welded by alternating current. They also reported a better mechanical behavior for samples welded by pulse current. In a study, Liu and Dongg [17] examined the AZ31 alloy welding by tungsten gas arc method and without the use of a filler metal. They found that the microstructure of the welding metal and the heat-affected region in the GTA method is different from the GTAF method, which changes the fracture site in the tensile test and improves the ultimate tensile strength of the

welded zone. According to their report, the grain size in the HAZ region in the sample welded with a filler metal shows less variation than the sample welded without the filler metal. This is due to the presence of the filler metal, which reduces the maximum temperature of the welding pond and decreases the energy transfer from the FZ to the HAZ area. Hasani et al. [18] studied the effect of the FSP on the microstructure and mechanical properties of the AZ91C magnesium cast alloy welding site. Their results showed that the FSP increases the mean micro-hardness value and leads to an increase in the distribution of micro-hardness uniformity from the weld metal side toward the base metal. Increasing hardness by applying various processes and creating work hardening on the surface during the abrasion test followed by reaching the stable state at the wear rate was introduced as the reason for improving the wear properties.

The attempts are today continuing to create a suitable joint for magnesium alloys. Given that we found no study on the improvement of the mechanical and microstructural properties of AZ31 cast alloy joint using the friction stir process in the scientific texts, adequate research should be done in this area to achieve the desired results. This paper was focused on examining the effect of FSP on the microstructure and the mechanical behavior of the welding zone of the AZ31 cast alloy joint.

Experimental procedure

In this study, the AZ31 magnesium cast alloy (prepared by sand casting method) was used as the base metal. The chemical composition of the magnesium alloy used in this study is presented in Table (1-3). The AZ31 magnesium plates with a size of $12 \times 75 \times 200 \text{ m}^3$ were cut using the waterjet. The samples were then prepared to perform the TIG welding process as Double-V Butt joint (X-shaped) with a 90° bevel angle using a milling machine and a coolant. Figure (1-3) illustrates a view of the connection design with its specifications.

Table 1. The chemical composition of the base metal and filler metal in this study based on the weight percentage (WT%).

Elements	Magnesium	Aluminum	Manganese	Zinc	Nickel
Base metal-AZ31	Base	2.8	0.32	0.86	0.001
Metal filler-AZ91	Base	8.6	1.5	0.25	0.14

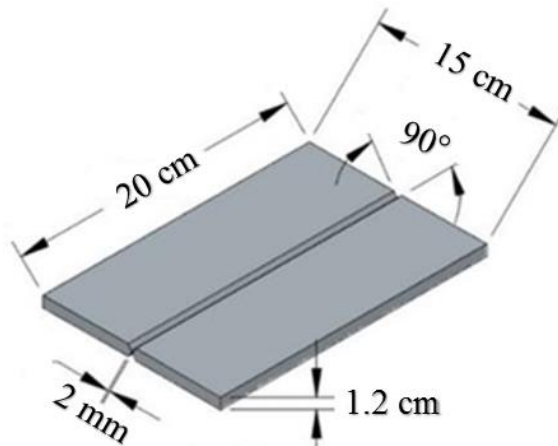


Fig. 1. A view of the connection scheme for use in the GTAW process.

The connection between casting magnesium alloys (AZ31) was done by tungsten-gas arc welding (GTAW) method using a tungsten electrode with a diameter of 2.4 mm and the AZ31 filler metal with a diameter of 3.2 mm. The connection of base metals was made with a DCEN current polarity, a root gap of 2 mm, a root face of 1.5 mm, and the preheating temperature of 200 °C. The prepared samples were cleaned with acetone before the welding and the cleaning process was done with a wire brush between each pass as well. The welding process was performed using the GAM Electric Welding Machine, PSQ 400A model with a water-cooling system under the argon gas with a

purity of 99.999% and a speed of 12 liters per minute. The parameters used in this process are presented in Table (2-3).

The frictional stir process was done to improve the microstructure and, consequently, the mechanical behavior of the junction in a pass on the welding line of the welded samples at a tool rotation speed of 1120 rpm, the tool traverse speed of 50 mm/min, and the instrument tray slope of 2 °. Also, the tool immersion depth within the sample surface was considered as 2 mm. The image of the Friction Stir Process (FSP) on the welding line of the samples is shown in Fig. 2.

Table 2. The welding parameters of the GTAW process.

Welding speed (mm/s)	Voltage (V)	Equivalent current (A)	Pulse time (sec)	Low current (A)	Peak current (A)	Parameter
2.5	12	187.5	0.5	125	250	Pass 1
2.5	12	187.5	0.5	125	250	Pass 2
2.5	12	187.5	0.5	125	250	Pass 3

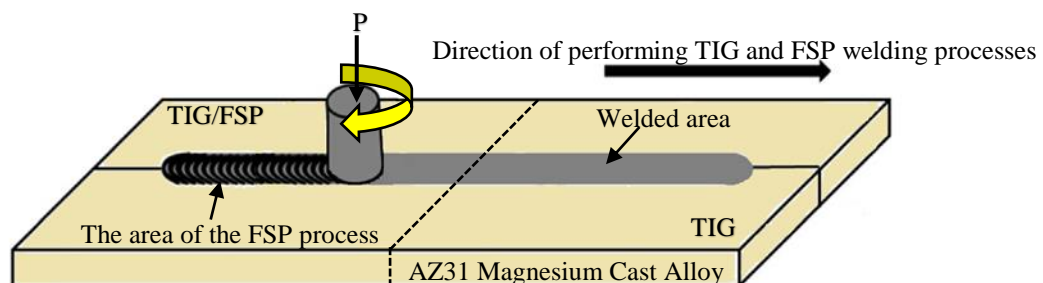


Fig. 2. A schematic view of the two welding process and the next FSP process used in this study.

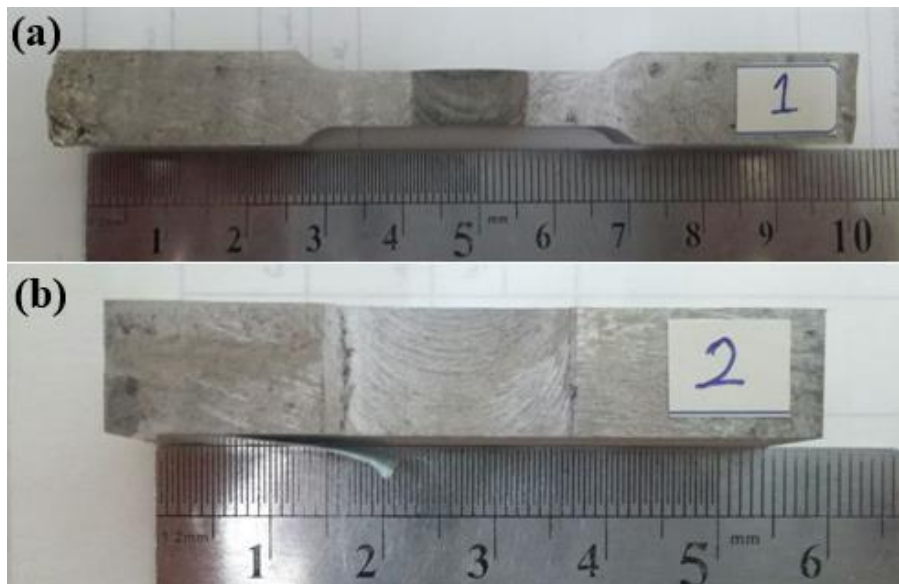


Fig. 3. A view of samples (a) tensile test (b) impact test.

The metallographic test and mechanical tests, including the tensile test, the micro-hardness measurement test, and the impact test were used to examine the microstructure of different welding regions and mechanical properties and the effect of FSP on the microstructure and mechanical behavior of the welded sample. The SEM was used for analysis of the fracture surfaces in the samples of tensile and impact tests. To this end, after performing the connection process, the samples with dimensions of $10 \times 55 \text{ mm}^2$ were provided. Using the sandpaper from 80 to 2500 series, a preparation process was done on them. Finally, the samples were polished with the diamond paste. The Picral Etchant solution (containing 10 ml acetic acid + 10 ml distilled water + 70 ml ethanol + 4.2 ml picric acid) was used for 3 to 8 seconds to examine the microstructure and changes in the different regions of the joint. The imaging of the microstructure of different regions was done using the SA-Iran optical microscope, Model IM 420, made in Iran, available at Islamic Azad University, Najaf Abad Branch. Also, the fracture cross-section of the samples in the tensile and impact tests was examined using the scanning electron microscope, the LEO 435VP model, equipped with the EDX analysis. The tensile, impact, and micro-hardness measurement tests were used to investigate the mechanical behavior of the joint and the effect of FSP on the mechanical

properties of welding. The tensile test was performed transversely and perpendicular to the welding line according to ASTM E8 standard with a 30-ton tension measurement machine, INSTON-4486 model, made in UK [19]. The Vickers micro-hardness test was performed according to ASTM E 92 standard by Vickers hardness method with the Tamping Diamond Pyramid by the Shimadzu micro-hardness meter, Model M. In this test, a force of 100 grams for 10 seconds was used at 1 mm intervals for both horizontal and vertical modes [20]. Also, the impact energy of the welded and processed samples was measured according to ASTM E23-00 standard [21]. This test was done using a SIT-300 Santam Impact Tool and at the ambient temperature. Figure 3 shows the view and the dimensions of the tension and impact samples.

Results and Discussion

The microstructure of the metal base of the AZ31 casting magnesium alloy with a magnification of 200X is presented in Fig. 4. The microstructure of the AZ31 alloy casting sample contains a lot of gas porosity. These defects occur due to the high tendency of magnesium to absorb hydrogen during melting and freezing. In fact, the hydrogen absorbed during the melting process of magnesium is released during freezing, and ultimately forms as porosity in the final frozen structure [22].

According to Fig. 4 (a), one can see that the microstructure is like large-dendritic grains of α -Mg. These dendrite grains typically grow under sand casting conditions due to the low traverse rate. Figure 4 (b) shows the results of the XRD analysis of the base metal. The XRD analysis results of the base metal indicate the presence of reticular coarse and continuous sediments of $Mg_{17}Al_{12}$ in the structure of AZ31 cast alloy. The distribution of sediment mainly occurs in the grain boundaries and partly within the grains. The $Mg_{17}Al_{12}$ phase is formed in the subsequent freezing stages due to its low melting point. There is also a dendritic structure at the base metal surface of the AZ31 cast magnesium alloy. Ren et al. [23] also observed a similar structure in their research.

Fig. 5 shows the microstructure of different regions of the AZ31 magnesium alloy welded by the TIG method. As shown in Fig. 5, the microstructure of this sample consists of several regions such as the base metal, the HAZ zone, and the welding metal. The size of the grains has increased in the microstructure of the zone affected by the heat (HAZ) compared to the base metal. According to Fig. 5 (c), the grains have slightly grown in the heat-affected zone (HAZ). No region with overheated microstructure compared with the base metal microstructure (BM) was seen, which is due to the use of the AZ91 filler metal. The AZ91 filler metal has

reduced the excess temperature in the melting pool and changed the thermal cycle of the HAZ area. As seen in Fig. 5c, in the heat affected zone, the formed sediments (phase β) along the grains boundary have had a coaxial growth, which is due to the rapid cooling rate of the weld. The sediments (phase β) formed on the grains boundary limit the grains growth and reduce the chance of the melting cracking of the HAZ area. In other words, the sediments (β phase) formed in the intersection of the welding metal with the base metal have grown along the sediments (β phase) present in the context of the base metal (α phase). This kind of growth, which is useful for the weld, is called epitaxial growth that links the weld zone to the base metal grains and reduces the concentration of stress in the intersection of the weld and the HAZ [24].

It is shown in Fig. 5 that the microstructure in the weld zone (WZ) appears as highly fine coaxial grains are along with sediments with an intermetallic $Mg_{17}Al_{12}$ composition (phase β). Due to the high rate of cooling in welding compared to casting, the welding metal has become more fine-grained than the base metal. Also, the formation of fine microstructure can be attributed to the high cooling rate due to good thermal conductivity and low heat capacity of magnesium that disturbs the growth of the grains in the weld zone [17].

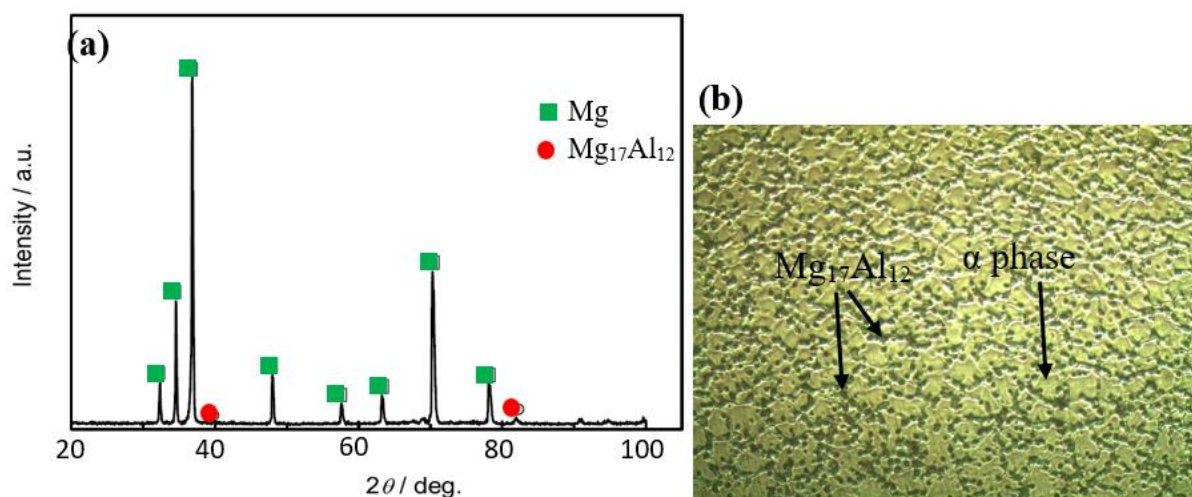


Fig. 4. (a) XRD analysis, (b) The microstructure of the base metal of AZ31 magnesium.

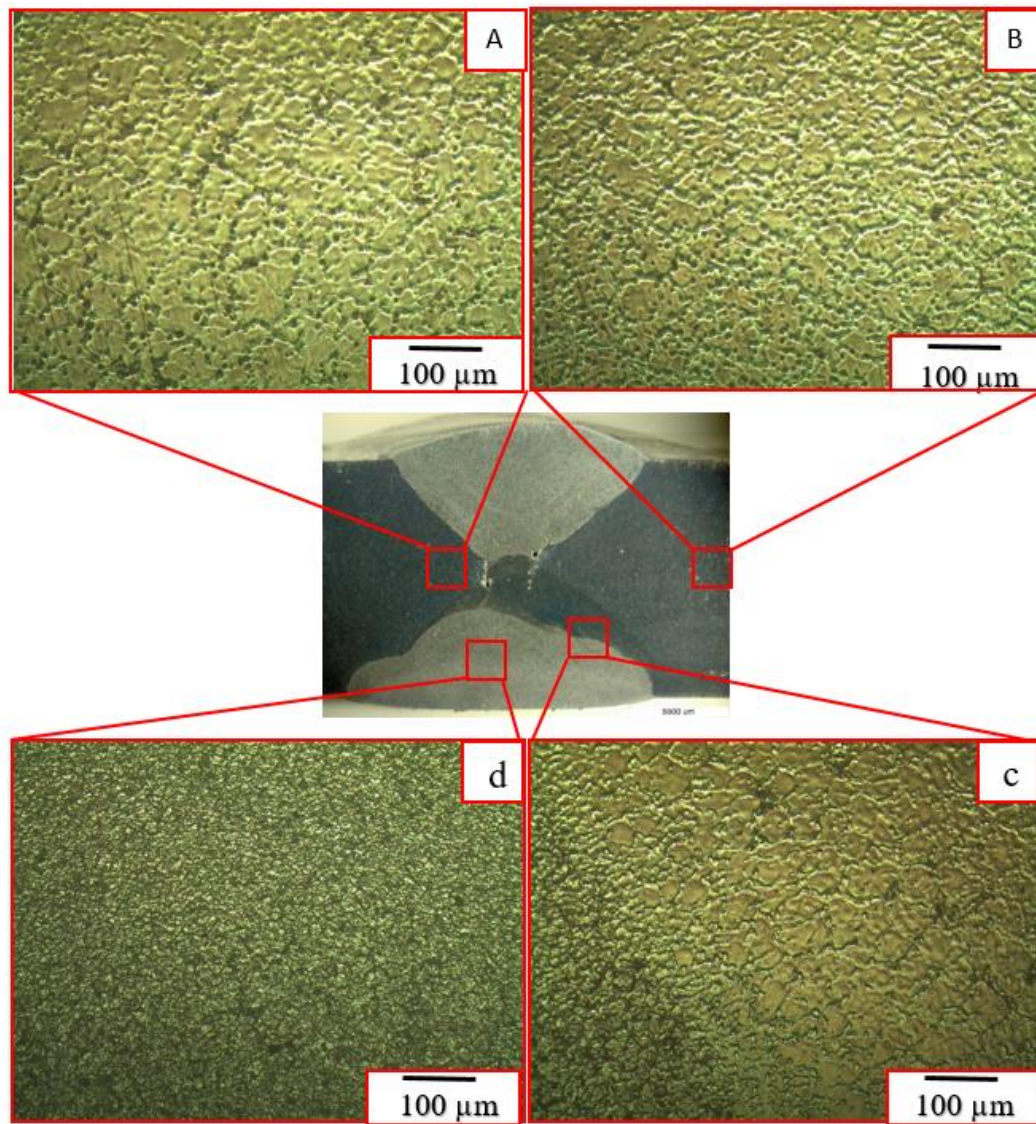


Fig. 5. The microstructure of different regions: (a) Base metal, (b) HAZ area, (c) HAZ-WM intersection, and (d) AZ31 magnesium alloy weld metal welded by TIG method.

Fig. 6 shows the microstructure of different regions of the AZ31 magnesium alloy welded by the TIG method and the subsequent FSP. As seen in Fig. 6, this sample has a more different structure than the TIG sample. According to Fig. 6, one can see that the joint has different regions, including the AZ31 base metal, the heat-affected zone (HAZ), the thermo-mechanically affected zone (TMAZ), and the weld nugget zone (WNZ). As can be seen, the fingerprint (onion-shape) region at the center of the weld is observed on both sides of the joint, which is due to the thermomechanical effects and various metallic flows. According to Fig. 6, it is seen

that the grains of the HAZ region have become more fine-grained than the base metal due to the heat generated by the friction. The fine-grained process is also seen in the TMAZ region. The transition areas between the WNZ and BM are the thermo-mechanically affected zone (TMAZ) with more stretched grains and the heat affected zone. The metallographic images from different regions of the TIG sample showed a highly fine and coaxial microstructure, including the sediments of $Mg_{17}Al_{12}$ secondary phase in the magnesium context (α phase). However, by applying the FSP process, the microstructure fine-graining and the β phase dissolution followed by the homogenization of the microstructure in the weld area would occur.

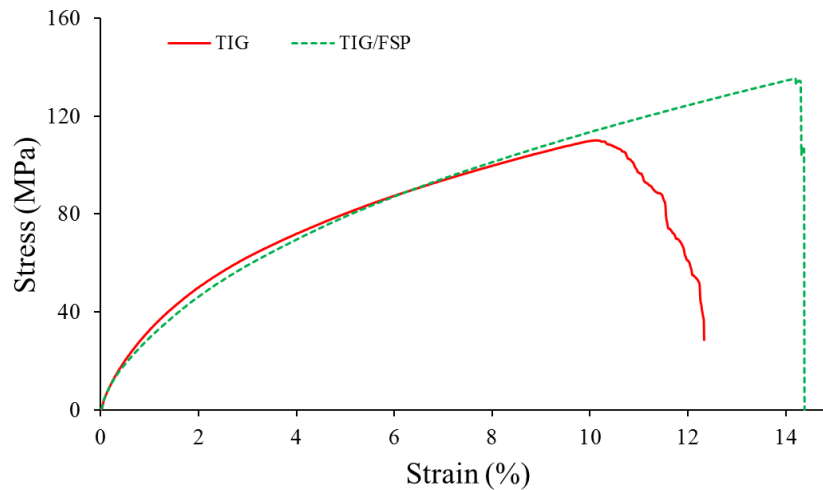


Fig. 7. Tensile test results for the welded samples.

Table 2. Tensile test results for the welded samples.

Sample No.	Tensile strength (MPa)	Yield strength (MPa)	Length increase (%)	Maximum applied force (N)
TIG	110.06±4	28.52	12.33±0.5	7924.59 ±50
TIG/FSP	135.34±5	9.51	14.39±0.4	9744.67±30

Figure 8 shows the image of the failure cross-section of the TIG and TIG/FSP samples. As shown in Fig. 8, the failure in the TIG/FSP sample has occurred from the intersection area of the welding metal and the heat affected zone. However, in the TIG sample, the failure has occurred in the weld area due to the presence of contractive cavities on the surface of the weld. As shown in Fig. 8a, the fracture surface has fine dimples and cavities. The presence of fine dimples and funnel-shape cavities in the fracture surface indicates that the failure has occurred quite softly. According to the results, the failure occurs softly in the TIG/FSP sample; however, in this sample, the size and number of cavities have greatly reduced as a result of the friction stir process compared to the TIG sample and the dimples have also become much finer.

Figure 9 shows the micro-hardness profile in the TIG and TIG/FSP samples. As can be seen, the micro-hardness in the base metal of the AZ31 casting magnesium alloy is approximately equal to 80 Vickers, which is confirmed by previous studies [27]. As shown in Fig. 9, the TIG micro-hardness has greatly increased in the welded

sample. The trend of increasing micro-hardness in the TIG sample is as follows: It initially increases with a very slight slope in the HAZ area, and after entering the weld region, the micro-hardness increases very strongly and reaches an average of 190 Vickers in the welding zone. The reason is the dramatic fine-graining of the microstructure in the weld area compared to the casting base metal. According to the results obtained in the microstructure, it was observed that the secondary phase sediments of $Mg_{17}Al_{12}$ are present in the TIG sample in the magnesium context (α phase), which is a crude and hard phase as the FSP process has reduced the micro-hardness in the weld region of the TIG sample. As can be seen, the micro-hardness has dropped by about 25% after completing the FSP process. By applying the FSP process on the welded sample by the TIG method, the phase β is dissolved in the context followed by the homogenization of the microstructure in the weld area. This has led to a loss of the micro-hardness in the weld area and an increase in the toughness of the TIG/FSP sample.

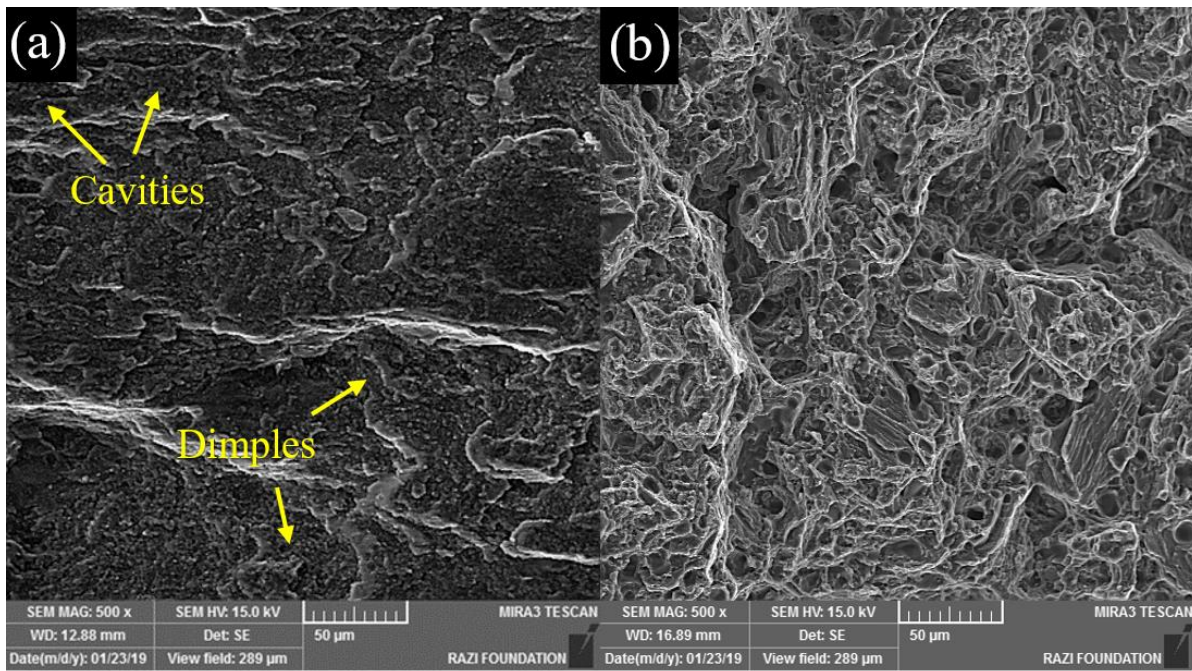


Fig. 8. The failure mapping of the failure surfaces of samples (a) TIG, (b) TIG/FSP.

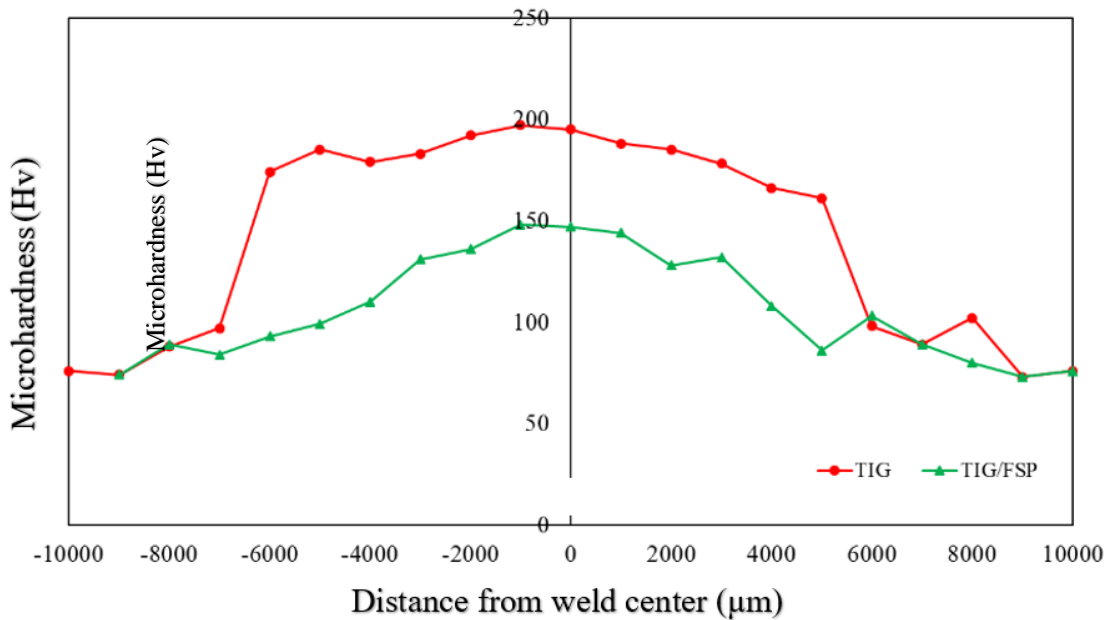


Fig. 9. The micro-hardness profile and the microstructure changes in the welded samples.

The vertical micro-hardness measurement test was used to investigate the micro-hardness in each of the welding passes and the effect of the FSP on the microstructure of each pass and compare the micro-hardness of different passes in the welding samples. Figure 10 shows the vertical micro-hardness values from the welding surface to the welding center point. As shown in

Fig. 10, the micro-hardness is reduced in the center of the TIG sample, which is due to the double-sided joint design. As seen in the TIG/FSP sample, the micro-hardness has increased in a zigzag pattern. This can be attributed to the effect of heat generated by the back pass of the FSP process.

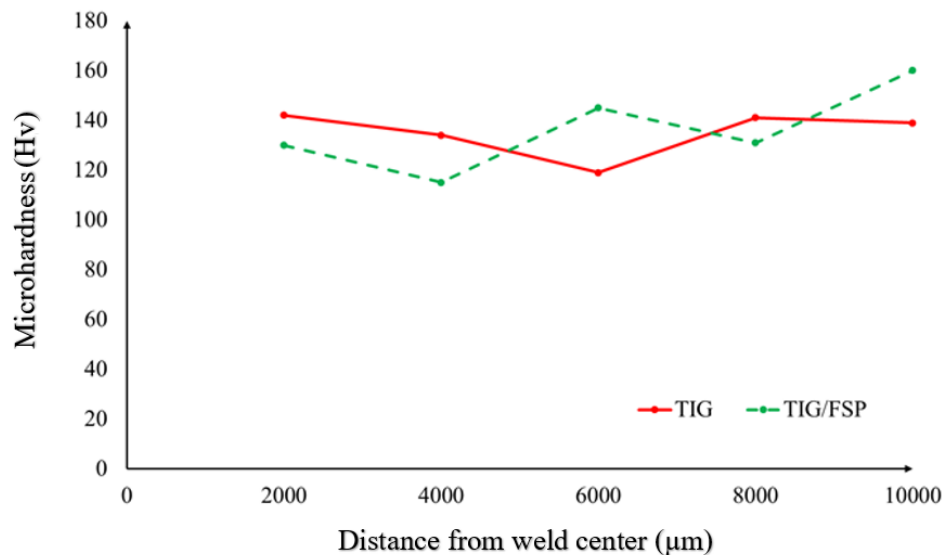


Fig. 10. The vertical micro-hardness profile from the welding surface to the other side of the weld

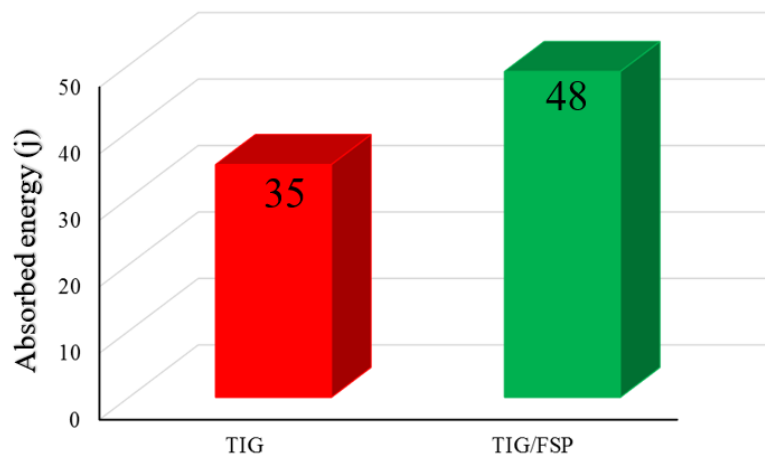


Fig. 11. The diagram of the rate of energy absorbed by the impact test.

The Charpy impact test of the welded samples was done according to the ASTM E23 standard at ambient temperature. The mean impact energy values of the weld metal in the TIG and TIG/FSP samples are presented in Fig. 11. As shown by the results, the impact energy values of the TIG and TIG/FSP samples are equal to 35 and 48 Jules, respectively. Following the performing of the friction stir process on the TIG sample, the impact energy increased by 37%. As the results show, the impact energy has improved after the friction stir process. These results indicate the improved microstructure in the weld metal. After the FSP, the fragile phase of β -Mg₁₇Al₁₂ and the secondary hard phases in the welding zone are dissolved in the grains, which increases the toughness. The obtained

results are completely consistent with the results of micro-hardness.

Since the values obtained in the results of the impact test of the welding metal are different, the fracture surface of the welding metal of the samples were examined by scanning electron microscopy. The morphology of the failure of the welding metals of TIG and TIG/FSP samples is presented in Fig. 12. As seen in Fig. 12, the failure is of a soft type in both samples. As can be seen, in the failure in the TIG-welded sample, the dimples are formed coarsely and stretched at the fracture surface. But with the reduction of microstructure size and decreasing the cavities and defects caused by welding by the FSP process, a soft failure occurs with fine dimples and funnel-shaped cavities.

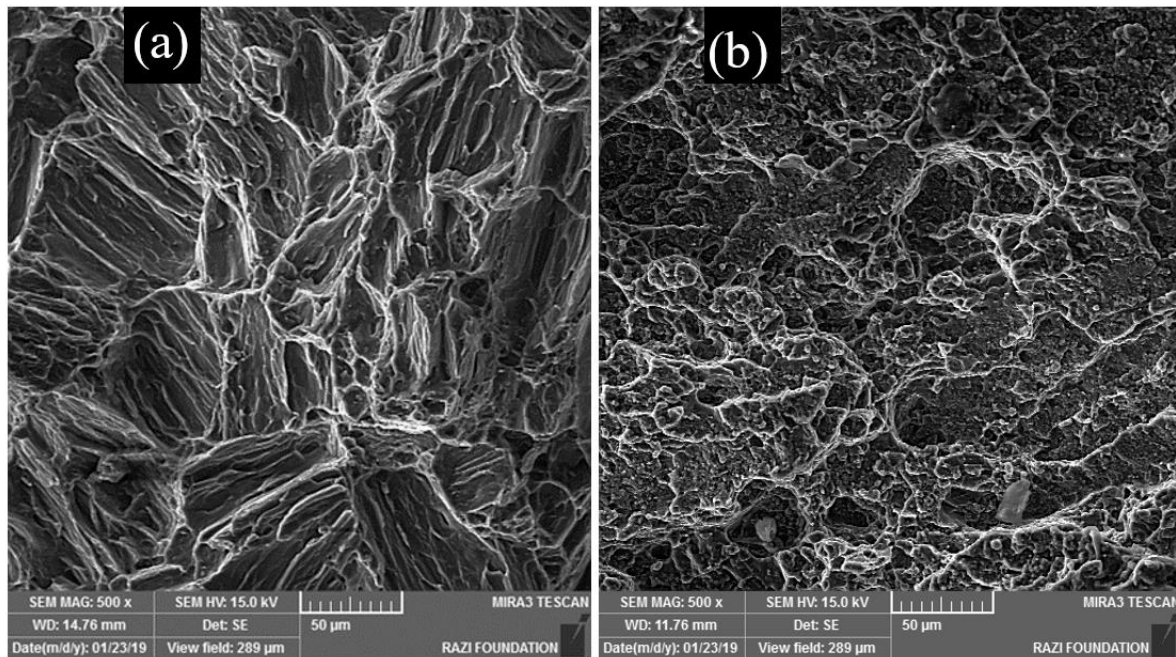


Fig. 12. Failure mapping of the fracture surface of the samples (a) TIG, (b) TIG/FSP.

Conclusions

In this paper, we evaluated the effect of the friction stir process on the microstructure and the mechanical behavior of the AZ31 casting alloy joint and the following results were obtained:

1. The microstructure of the welding metal of the TIG sample was formed highly fine and rough. After performing the process on the TIG sample, the morphology of the weld region was seen in an onion-shape form. The FSP resulted in the uniformity and homogeneity in the microstructure of the TIG sample weld by dissolving the crude and coarse phases of β - $Mg_{17}Al_{12}$, the dendritic microstructure of the TIG weld area, and the recrystallization of the grains.
2. The tensile strength in the TIG and TIG/FSP samples is equal to 110.06 and 135.34 MPa, respectively. After performing the FSP on the TIG sample, the tensile strength increases by 23%.
3. The impact energy of TIG and TIG/FSP samples was obtained as 35 and 48 Jules, respectively. After performing the FSP, the impact energy has improved by 37%.

4. The micro-hardness has reduced by about 25% after the FSP. By applying the FSP on the welded sample by the TIG method, the phase β is dissolved in the context (field) followed by the homogenization of the microstructure in the weld area. This has led to a loss of micro-hardness in the weld region and the increased toughness of the TIG/FSP sample.
5. The microstructural and mechanical results indicated that the FSP improves the microstructure and the mechanical behavior of the AZ31 casting alloy welding zone.

References

- [1] S.M. Chowdhury, D.L. Chena, S.D. Bhole, X. Cao, "Tensile properties of a friction stir welded magnesium alloy: Effect of pin tool thread orientation and weld pitch", *Mater. Sci. Eng. A*, Vol. 527, 2010, pp. 6064–6075.
- [2] D. Sameer Kumar, C. Tara Sasanka, K. Ravindra, K.N.S. Suman, "Magnesium and Its Alloys in Automotive Applications – A Review", *Mater. Sci. Technol.* Vol. 4, 2015, pp. 12-30.
- [3] N. Winzer, P. Xu, S. Bender, T. Gross, W.E.S. Unger, C.E. Cross, "Stress corrosion cracking of gas-tungsten arc welds in

- continuous-cast AZ31 Mg alloy sheet” *Corros. Sci.*, Vol. 51, 2009, pp. 1950-1963.
- [4] Ch. Moosbrugger, *Introduction to Magnesium Alloys, Engineering Properties of Magnesium Alloys*, ASM International, USA, 2017, pp. 148.
- [5] European Committee for Standardization, *Magnesium and Magnesium Alloys-Magnesium Alloy Ingots and Castings*, ISO, 1997, pp. 113.
- [6] M. M. Avedesian, and Hugh Baker., *Magnesium and magnesium alloys*”, ASM International, Handbook Committee, 1999, pp. 210.
- [7] A. Kennedy, A. Sollars, “Magnesium and aircraft engineering”, *Aircr Eng Aerosp Tech.*”, Vol. 82, 2010, pp. 267-273.
- [8] A. Luo, M. O. Pekguleryuz, “Cast magnesium alloys for elevated temperature applications”, *Jou. Mater. Sci.*, Vol. 29, 1994, pp 5259–5271.
- [9] V. Jain, R.S. Mishra, A.K. Gupta, “Study of β -precipitates and their effect on the directional yield asymmetry of friction stir processed and aged AZ91C alloy” *Mater. Sci. Eng. A*, Vol. 560, 2013, pp. 500–509.
- [10] M. Fairman, N. Afrin, D.L. Chen, X.J. Cao, M. Jahazi, *Can. Metall. Q.*,”Microstructural Evaluation of Friction Stir Processed AZ31B-H24 Magnesium Alloy”, *Can. Metall. Quart.*, Vol. 46, 2007, pp. 425–432.
- [11] B.M. Darras, M.K. Khraisheh, F.K. Abu-Farha, M.A. Omar, “Friction stir processing of commercial AZ31 magnesium alloy”, *Mater. Proc Technol*, Vol. 191, 2007, pp. 77–81.
- [12] B. Darras, E. Kishta, “Submerged friction stir processing of AZ31 Magnesium alloy”, *Mater. Desig.*, Vol. 47, 2013, pp. 133–137.
- [13] M. Gao, Sh. Mei, Z. Wang, X. Li, Xiaoyan Zeng, “Process and joint characterizations of laser–MIG hybrid welding of AZ31 magnesium alloy”, *Jou Mater Proc. Technol*, Vol. 212, 2012, pp. 1338-1346.
- [14] Y. N. Zhang, X. Cao, S. Larose and P. Wanjara, “Review of tools for friction stir welding and Processing”, *Can Metall Quart.*, Vol. 51, 2012, pp. 250-261.
- [15] R. S. Mishra, Z. Y. Ma, “Review paper-friction stir welding and processing,” *Mater Sic Eng.*, Vol. 50, 2005, pp. 1-78.
- [16] B. Demir, Karabuk, and A. Durgutlu, “An Investigation of TIG Welding of AZ31 Magnesium Alloy Sheets”, *Mater Test Weld Appl.*, Vol. 56, 2014, pp. 847-851.
- [17] L .Liu, Ch. Dong, “Gas tungsten-arc filler welding of AZ31 magnesium alloy”, *Mater. Lett.*, Vol. 60 , 2006, pp. 2194–2197.
- [18] B. Hassani, F. Karimzadeh, M. H. Enayati, S. Sabooni, and R. Vallant, “Effect of Friction Stir Processing on Microstructure and Mechanical Properties of AZ91C Magnesium Cast Alloy Weld Zone”, *Mater. Engin. Perf.*, Vol. 5, 2016, pp. 2776-2785.
- [19] ASTM E8-00 Standard Test Methods for Tension Testing of Metallic Materials.
- [20] ASTM E92-82 Standard Test Method for Vickers Hardness of Metallic Materials.
- [21] ASTM E23-02 Standard Test Methods for Notched Bar Impact Testing of Metallic Materials.
- [22] F. Y. Lan, H. M. Chen, W. P. Guo, J. Zhang and Y. X. Jin, “ Effects of Friction Stir Processing on Mechanical Properties and Damping Capacities of AZ31 Magnesium Alloys”, *Mater Sci Eng.*, Vol. 230, 2017, pp. 1-5.
- [23] Zh. Ren, X. Zhang, H. Hao, L. Sui, T. Zhang and Y. Ma, “Microstructures and mechanical properties of AZ31-0.1Ca magnesium alloy produced by soft-contact electromagnetic casting and hot extrusion”, *Acta Metall. Sin.*, Vol. 23, 2010, pp90-98.
- [24] B. Sadeghi, H. Sharifi, M. Rafieia, M. Tayebi, “ Effects of post weld heat treatment on residual stress and mechanical properties of GTAW: The case of joining A537CL1 pressure vessel steel and A321 austenitic stainless steel”, *Eng Fail. Analy*, Vol. 94, 2018, pp. 396–406.
- [25] S. Ramesh Babu, V.S. Senthil Kumar, G. Madhusudhan Reddy, L. Karunamoorthy, “Microstructural Changes and Mechanical Properties of Friction Stir Processed Extruded AZ31B Alloy”, *Procedia Engineering*, Vol. 38, 2012, pp. 2956-2966.
- [26] A. Sik, “Comparison between microstructure characteristics and joint performance of AZ31 magnesium alloy welded by TIG and friction stir welding (FSW) processes”, *Kovove Mater.*, Vlo. 51, 2013, pp. 197–203.
- [27] Z. Da-tong, X. Feng, Z. Wei-wen, Q. Cheng, Z. Wen, “ Super plasticity of AZ31 magnesium alloy prepared by friction stir processing”, *Trans. Nonferrous Met. Soc. China*, Vol. 2011, pp. 1911-1916.